GLOBAL NAVIGATION SATELLITE SYSTEM REFLECTOMETRY (GNSS-R) ALGORITHMS FOR WETLAND OBSERVATIONS

Cinzia Zuffada, Clara Chew, Son V. Nghiem

Jet Propulsion Laboratory, California Institute of Technology, Pasadena, CA, USA

ABSTRACT

It is important to closely monitor the state of the world's wetlands, as climate change and human encroachment in a rapid global urbanization trend threaten to cause large-scale wetland collapse. Because wetlands are often difficult to observe *in situ*, remote sensing is the only viable way to map wetland extent globally. However, current remote sensing methods suffer limitations in capturing wetland extent, and more importantly, wetland dynamics at appropriate spatial and temporal scales. GNSS-Reflectometry could help fill the current observation gap, as experimental data show that ground-reflected GNSS signals are very sensitive to changes in inundated areas. Furthermore, because this technique only requires a custom developed receiver and antenna system, a constellation of such instruments can potentially be launched at relatively low cost, providing global observations at sub-daily intervals. One challenge remains, however, which is quantitatively formulating the geophysical product of reflections over the land surface in various states of inundation. Here, we use a novel reflection dataset, derived from the SMAP radar receiver, to elucidate the sensitivity of reflections to small land surface features and their seasonal variations. Additionally, we quantify the dynamic range of reflections over both open and closed wetlands, and suggest an algorithm for wetland type classification.

Index Terms— wetlands, remote sensing, GNSS, reflectometry, SMAP radar receiver

1. INTRODUCTION

Wetlands are areas that are inundated or saturated either permanently or intermittently, and that support vegetation types adapted to saturated conditions. Wetlands provide several ecosystem services like flood mitigation and support a vast array of flora and fauna that are unique to wetland areas. Water stored in wetlands is an important component of terrestrial water storage, as it affects not only local hydrology and ecosystems, but also surrounding floodplains. Wetlands play a significant role in the emission of global atmospheric methane (CH_4) that is 25 times stronger than carbon dioxide (CO_2) as a greenhouse gas on the centennial time scale [1]. Community reports state that among the multitude of methane emission sources, wetlands constitute the largest contributor (30% of total) and also have the widest uncertainty range, hindering climate change projections [1]. Yet, knowledge of wetland extent and dynamics is limited since existing observational techniques cannot adequately resolve the spatial and temporal scales necessary to produce dynamic maps of global wetland extent over multiple decades. The rapid rate of wetland collapse demands urgent attention, not only for methane emission but also for the impact to water cycle and for sea level change assessments.

Recently, Nghiem et al. [2] have demonstrated that the GNSS-R observations from aircraft and satellites can identify inundated areas under varying vegetation cover, including a dense rice canopy and a thick forest with tall trees, where optical sensors and monostatic radars have limited capabilities. Specifically, by analyzing GNSS-R data acquired from the Technology Demonstration Satellite (TDS-1) and from a 2005 aircraft experiment over the Ebro delta in Spain [3], it is shown that the reflections over wetlands have a very strong coherent component and the peak values are several dB higher (even reaching 10 dB, equivalent to one order of magnitude) than those over surrounding dry lands. When reflections are coherent, the contributing area to the peak power is approximately equal to the first Fresnel zone, which for low Earth orbiting satellites is less than a kilometer. Unfortunately, since the TDS-1 reflection experiment was not designed for land surface remote sensing, the data available to the research community has been averaged spatially over ~ 7 km along the satellite track, thus making it difficult to elucidate the true spatial resolution of each reflection.

Following the malfunction of the SMAP radar transmitter in 2015, the SMAP project agreed to retune the receiver's bandpass center frequency to 1227.45 MHz. in an experiment to collect GPS L2C (reflected) signals, which are transmitted by approximately half of the GPS satellites. The SMAP radar receiver has a bandwidth of 1.25 MHz each for the horizontal (H) and vertical (V) polarized channels. The GPS reflection data recorded by the SMAP radar receiver comprises a unique experimental dataset, with its own advantages and challenges. The data provide an excellent opportunity to test the spatial sensitivity of reflections, particularly because a) the high gain of the SMAP radar antenna of ~ 36 dB ensures signal level much higher than noise; b) the antenna pattern does not vary within the area of collection; and c) the geometry of each bistatic scattering path has a constant incidence angle of ~ 40 degrees. However, since the SMAP radar antenna is rotating with periodicity of ~ 4 s, any one specular reflection point remains within its main beam for a very short period of time. Hence, the cross-correlation process was limited to a 25-ms window approximately centered on the beam's closest approach to the specular point. Five 5-ms coherently-integrated waveforms were then incoherently summed in power to increase the SNR. The short integration time provides additional capability to test the spatial resolution of the reflection, though the rotating antenna means that each reflection is approximately 25 km apart from the subsequent one.

In this study, we examine reflection data derived from the SMAP radar receiver and TDS-1 in order to more fully understand the ability of GNSS-R to differentiate changes in small landscape-scale features and assess quantitatively how wetland types might be classified based on the signal level.

2. METHODS

2.1 Phenomenology - GNSS-R data are produced in the form of delay-Doppler maps (DDMs), which represent the two-dimensional cross-correlation between the received (reflected) signal and a locally-generated replica signal. An example DDM corresponding to reflections over wetlands is shown in Fig. 1.

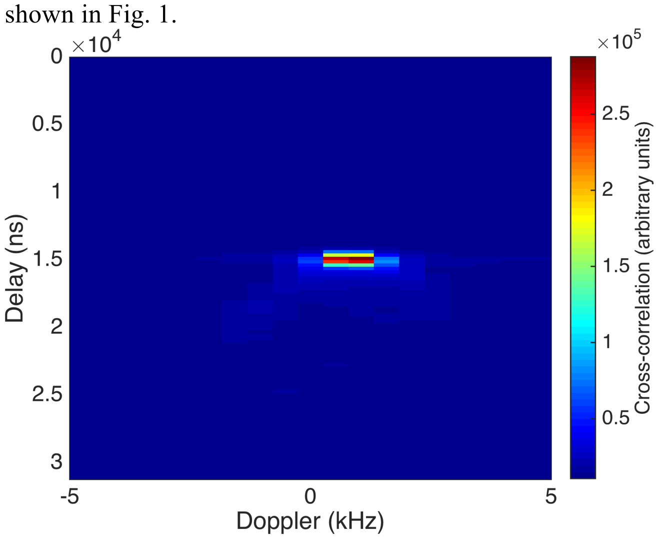

Figure 1. DDM over wetlands, showing very narrow spreads in delay and Doppler, associated to the coherent nature of the scattering.

In order to summarize spatial features and temporal changes in DDMs over wetlands, the main metric to consider is the signal-to-noise ratio (SNR). The peak value will be affected by the dielectric constant of the reflecting surface, underlying medium and roughness, which will in turn determine the extent of coherence in the signal.

First, we analyze spatial differences over a flat salt pan in South America, Salar de Uyuni, which is often used for satellite calibration. As one of the flattest areas of the world, it is a good place to begin to analyze SMAP DDMs. We then compare DDM statistics from Salar de Uyuni and other flat lands to DDM statistics from open wetlands, which are areas of mostly calm water with little vegetation overgrowth. One would expect these areas to produce coherent reflections in calm or low-wind conditions. Finally, we analyze DDMs for areas of closed wetlands, which are inundated areas overgrown with a thick vegetation cover.

In these cases of closed wetlands, it is noted that the reflected coherent GNSS signal is significantly strong around the specular direction only, and the power density rapidly decreases away from it. The coherent scattering is assumed to come only from the reflected signals over the water, possibly attenuated by the vegetation canopy. On the other hand, incoherent scattering includes volume scattering from leaves and branches, contributions due to the soil and trunk interactions, multiple interactions between vegetation elements, and between the vegetation and the soil, and incoherent scattering from the soil attenuated by the overlapping vegetation canopy.

After comparing DDM statistics for flat lands, open wetlands, and closed wetlands, we test the applicability of the following equation to solve for the coherent reflectivity, formulated in [4][5]

$$P_{coh,p} = \Gamma_p \frac{P_t \lambda^2 G_t G_r}{(4\pi)^2 (R_t + R_r)^2} \qquad (1)$$

where $P_t G_t$ is the Equivalent Isotropic Radiated Power (EIRP) of the transmitted signal, G_r is the antenna gain of the receiver, and Γ_p is the reflectivity of the reflecting surface at a specified polarization p and at the observation geometry for GNSS-R. We expect the reflectivity to be attenuated by the presence of vegetation as in [5], and we investigate the extent of this attenuation in the closed wetlands.

2.2 Classification – Knowing that the presence of water is the primary factor contributing to the reflectivity of Eq. 1, a simple model based on changes in reflectivity can be developed to represent the change in SNR depending on the percentage of water in the measured reflected footprint in the Amazon wetlands, if we assume that the major source of reflectivity in the Amazon is coming from the water. To establish an estimation of the percentage of water within the reflected footprint, we used 25 m backscatter observations from PALSAR-2. Backscatter observations were analyzed to classify whether they represented open water, flooded vegetation, or vegetation only, using classification methods similar to those found in the radar use in hydrology literature A set of TDS-1 measurements contemporaneous and collocated with the PALSAR measurements (to +/- 15 days) were chosen to validate the model.

3. RESULTS

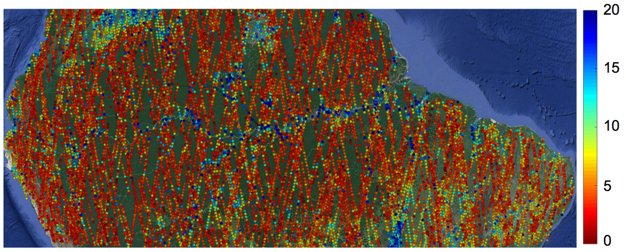

Figure 2: SNR at vertical polarization collected over the Amazon, for the period of Sep 2015 – Aug 2016.

Fig 2 shows the SNR of DDMs recorded over the Amazon. High SNR, which can be indicative of flat dry surfaces, wet surfaces, or both, is observed over and close to the Amazon River as well as the savannas in and around Tuparro National Natural Park in Colombia. Low SNR is observed over areas of high biomass in the Amazon, indicating a smaller degree of coherence or lack of coherence in these areas. High SNR is also observed over rivers with widths less than 50 m, an indication that the reflected signal is sensitive to surface features of sub-km scale.

The large dynamic range of the SNR is beneficial to investigate seasonal variations of wetlands extent, as exemplified in Fig 3 for the African continent. Here, we plot the gridded changes in peak SNR between summer 2016 and winter 2015/2016. The spatial pattern exhibits a strong seasonality, particularly over Central Africa, which is known to have different monsoon seasons north and south of the equator.

Figure 3. Observed changes in SMAP H-pol reflections peak SNR. The tropical regions, where most of the rainfall occurs, exhibit the largest changes, consistent with observations from traditional instruments.

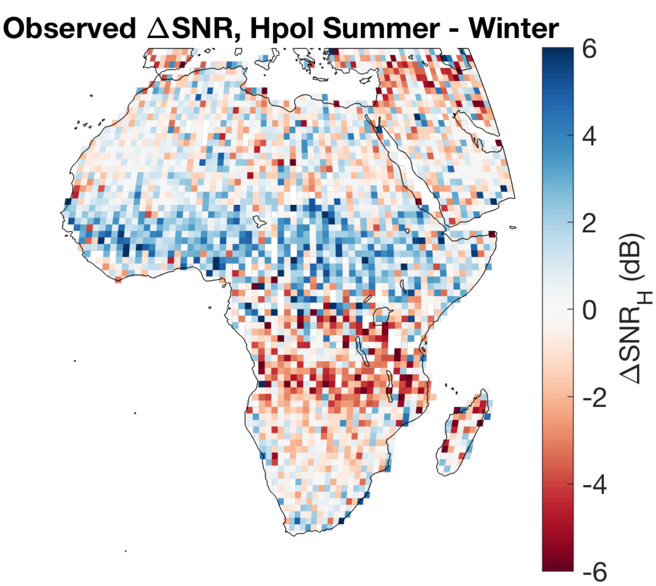

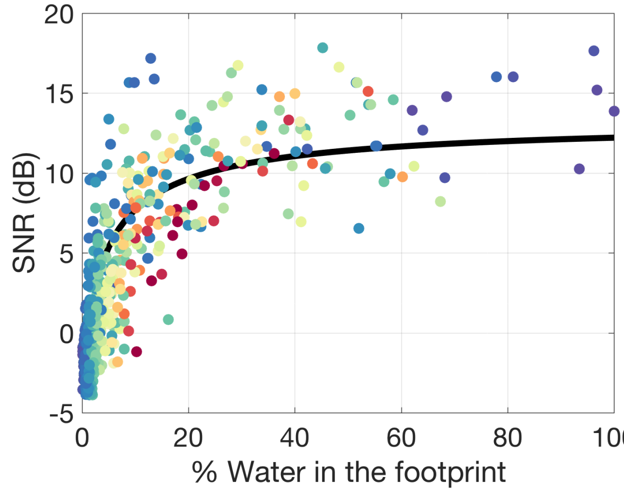

Figure 4. Comparison between modeled (black solid curve) and TDS-1 data of SNR range versus % of water in the data footprint for the Amazon wetlands. Color represents % of that water that is underneath vegetation (0 – blue; 10+ – red). The % of water in the footprint of the TDS-1 measurements was estimated with use of PALSAR-2 data.

Figure 4 illustrates the comparison between our model and TDS-1 data in the Amazon, showing the SNR distribution as a function of the percentage of water in the measured footprint, and highlighting the behavior for different amounts of that same water underneath vegetation. The simple model agrees quite well with the observations, and could be used as a Geophysical Model Function to generate an inundation product. Note that it also provides a first order quantitative assessment of the extent of attenuation of the bistatic reflections off vegetated wetlands in the Amazon region.

4. CONCLUSION

Analysis of DDMs over flat lands and open wetlands indicate a large dynamic range and coherence in the reflected signal, which support our assertion that in many regions, ground-reflected GNSS signals have a large sensitivity to small spatial features. Here we have shown that spaceborne GNSS-R is sensitive to many small-scale landscape features in areas of the Amazon open wetlands and wetlands with moderate vegetation cover. Additionally, a strong response to seasonal variation of Africa's tropical wetlands has been observed, consistent with the behavior of the monsoons. A wetlands classification algorithm has been proposed for the Amazon, which could lead to the generation of inundation products. Future work should include modeling the reflected signal over wetland areas to further establish the degree of signal coherence.

5. ACKNOWLEDGEMENT

This research was carried out at the Jet Propulsion Laboratory, California Institute of Technology, under a contract with the National Aeronautics and Space Administration. In particular, the research on urbanization and impacts by Nghiem was supported by the NASA Land-Cover and Land-Use Change (LCLUC) Program. Nghiem was also supported by the Advanced Concepts Program at JPL for wetland study. The authors would like to thank members of the SMAP team for retuning the SMAP receiver's recording bandpass and providing help with the Level-1 data format and antenna gain pattern. We would also like to thank Steve Lowe, Shadi Oveisgharan, and Stephan Esterhuizen for generating the SMAP reflection data. We acknowledge funding from the NASA Postdoctoral Program and the JPL internal Research and Technology Development Program.

6. REFERENCES

[1] IPCC (2013), Climate Change 2013: *The Physical Science Basis*, Contribution of Working Group I to the Fifth Assessment Report of the Intergovernmental Panel on Climate Change, Stocker, T.F., D. Qin, G.-K. Plattner, M. Tignor, S.K. Allen, J. Boschung, A. Nauels, Y. Xia, V. Bex and P.M. Midgley (eds.), 1535 pp., Cambridge University Press, Cambridge, United Kingdom and New York, NY, USA.

[2] Nghiem, S. V., C. Zuffada, R. Shah, C. Chew, S. T. Lowe, A. J. Mannucci, E. Cardellach, G. R. Brakenridge, G. Geller, and A. Rosenqvist (2016), Wetland Monitoring with Global Navigation Satellite System Reflectometry, *Earth and Space Science*, 3, doi:10.1002/2016EA000194.

[3] Cardellach, E., F. Fabra, O. Nogués-Correig, S. Oliveras, S. Ribó, and A. Rius (2011), GNSS-R ground-based and airborne campaigns for ocean, land, ice and snow techniques: application to the GOLD-RTR datasets, *Radio Sci.*, *46*, doi:10.1029/2011RS004683

[4] de Roo, R.D., and F.T. Ulaby (1994), Bistatic specular scattering from rough dielectric surfaces, *IEEE Trans. Antennas Propagat.*, 42(2), 220-231.

[5] Pierdicca, N., L. Guerriero, M. Brogioni, and A. Egido (2012), On the coherent and non coherent components of bare and vegetated terrain bistatic scattering: Modelling the GNSS-R signal over land, in *Proc. IEEE Int. Geosci. Remote Sens. Symp*., 3407-3410, 22-27 Jul., Munich, Germany.

[6] http://www.eorc.jaxa.jp/ALOS/en/palsar_fnf/fnf_index.htm